Intrapulse Recognition of Radar Signals Via Bicubic Interpolation WVD

ZI-LONG WU
XIANG-XUAN HUANG
MENG DU
XIN-SONG XU
DAPING BI
JI-FEI PAN
National University of Defense Technology, Hefei, China

In regards to electromagnetic warfare application, this work proposes a radar intrapulse recognition algorithm based on bicubic interpolation Wigner–Ville distribution (WVD). The proposed method is aimed at overcoming the complexity of traditional feature extraction and enhancing the robustness of intelligent intrapulse recognition systems. First, we convert the WVD matrices of radar intrapulse signals into square matrices using bicubic interpolation. This enables the intrapulse recognition algorithm to handle radar signals with varying lengths. Second, we use the square matrices directly to train a convolutional neural network (CNN), rather than first saving them as images and then training the network with those images. This is because automatic storage and retrieval of images can sometimes alter the numerical values in the matrices. We enhance the performance of the CNN by utilizing batch normalization and one-hot encoding techniques, and continuously evaluate the CNN during training to save the best performing model. Finally, we use the trained CNN to identify the intercepted radar intrapulses and verify the reliability of the proposed method based on the radar signals generated by hardware devices. The experimental results demonstrate that the proposed algorithm can recognize radar intrapulses with varying pulsewidths. Furthermore, the proposed algorithm exhibits strong recognition performance even at a low signal-to-noise ratio and has lower time complexity than the existing algorithms.

Manuscript received 21 September 2022; revised 18 January 2023, 26 April 2023, and 3 July 2023; accepted 18 August 2023. Date of publication 23 August 2023; date of current version 8 December 2023.

DOI. No. 10.1109/TAES.2023.3307665

Refereeing of this contribution was handled by D. A. Garren.

This work was supported in part by the National Natural Science Foundation of China under Grant 62071479, in part by the Independent Scientific Research Project of the National University of Defense Technology, and in part by the Postgraduate Scientific Research Innovation Project of Hunan Province under Grant CX20220032 and Grant CX20220014.

Authors' addresses: Zi-Long Wu, Xiang-Xuan Huang, Meng Du, Xin-Song Xu, Daping Bi, and Ji-Fei Pan are with the School of Electronic Countermeasures, National University of Defense Technology, Hefei 230031, China, E-mail: (wuzilong@nudt.edu.cn; 514910034@qq.com; 2501539040@qq.com; xuxinsong17@nudt.edu.cn; bdpeei@163.com; 22920142204021@stu.xmu.edu.cn). *(Corresponding author: Ji-Fei Pan).*

I. INTRODUCTION

In the field of electromagnetic warfare (EW) [1], [2], radar emitter recognition (REI) plays an essential role in electronic support measures (ESM) and electronic intelligence (ELINT) systems [3], [4], [5], [6]. The ESM system is responsible for understanding the radio frequency environment and providing emission intercept, detections, recognition, characterization, location, and overall situational awareness of emitters [7]. The purpose of the ELINT system is to provide information about threatening system, emitter tracking, threating assessment, and platform recognition [8]. With the large-scale application of complex radar systems in actual battlefields, the REI methods based on the traditional features are gradually becoming unable to meet the needs of new military missions, especially when only very short radar pulse sequences can be intercepted. Therefore, REI methods are expected to become more general and universal. In fact, the differences in radar emitters are often hidden in intrapulses. Therefore, to improve the reconnaissance capabilities of REI, the capability of intrapulse recognition (IPR) of radar signals should be improved. The IPR technology has gradually become the research focus of scholars worldwide as it can simply realize REI.

The intrapulse modulation used in early radars was simple. Therefore, pulse description words (PDW) of radar can be selected as features to identify different radar intrapulses [9], [10] PDW primarily includes the time of arrival, direction of arrival, carrier frequency, pulsewidth (PW), pulse amplitude, and pulse modulation. To improve the combat capability of one's own radar and weaken enemy interference, radar signal modulation needs to be gradually developed from simple modulation to complex frequency and phase modulation. Early radars mostly used conventional pulse (CP) signals. Then, continuous sine waves were mostly used in radar to measure the speed of the target. Linear frequency modulation (LFM) signals are mostly used in pulse Doppler radar to improve the Doppler resolution. Barker codes are widely used in pulse compression radar because Barker codes have ideal autocorrelation, which solves the contradiction between the distance resolution and speed resolution [11], [12]. Gaussian frequency-shift keying/phase-shift keying is an excellent signaling choice for low-probability intercept radar applications because of its increased bandwidth [13]. Hence, when implementing the IPR of radar signals, we can seek the help of radar signals modulation identification methods.

Additionally, the remarkable achievements of deep learning in the field of computer vision have led to intelligent advances in REI and IPR [14], [15], [16], [17]. To reduce the training time of the network and improve the stability of deep neural networks (DNNs), it is generally necessary to perform domain transformation processing on radar intrapulses first. In recent years, domain transformation has been widely used in the field of signal

recognition, mainly including short-time Fourier transform (STFT) [18], wavelet transform [19], Wigner–Ville distribution (WVD) [20], Hilbert–Huang transformation (HHT) [21], [22], Choi–Williams distribution (CWD) [23], and others. However, the initial matrices obtained by domain transformation are often not square matrices, which hinders the effective combination of domain transformations and DNNs. The dimensions of the initial matrices corresponding to various domain transformations are different, which makes it difficult to compare the feature expression capabilities of various domain transformations.

Furthermore, the same intrapulse can yield matrices with varying dimensions after undergoing different domain transformations, while intrapulses of different lengths can also yield matrices with varying dimensions even when undergoing the same domain transformation. In practice, some radars use wider pulses, such as pulse compression radars, to achieve greater detection range, resulting in different PWs between different radar emitters. These different PWs often lead to varying lengths of radar intrapulses. Moreover, during the interception of radar signals, the sampling points captured for the same pulse can differ due to varying sampling rate settings. Additionally, different radar signal receivers may be used to capture signals, and due to hardware differences, even the sampling points for the same pulse can differ. Furthermore, the trailing edge of pulses can be extended under the influence of multipath transmission channels, making PW measurements much noisier than lead edge measurements, such as pulse repetition interval.

Domain transformations, signal properties, and hardware equipment can all lead to variations in the dimensions of intrapulse samples that need to be recognized. These issues have hindered the development of IPR technology, especially under complex conditions [24], [25], [26], [27], [28], [29]. Therefore, addressing the issue of varying dimensions is crucial for IPR. Processing the samples with varying dimensions into samples with a fixed dimension would enable radar intrapulse samples of any dimension to be input into a DNN with a fixed input size. Then, we can use DNNs to recognize radar intrapulses.

It is noteworthy that bicubic interpolation can effectively scale matrices with varying dimensions to the desired dimensions while preserving the characteristics of intrapulse samples. Therefore, bicubic interpolation can be used to scale the varying dimensions of intrapulse samples resulting from radar pulses of different lengths and domain transformations, enabling samples of varying dimensions to be processed into fixed-dimension samples. These fixed-dimension samples can then be recognized using DNNs, as the input size of DNNs is generally fixed.

In this work, we propose an IPR algorithm via bicubic interpolation WVD. First, we collected some radar intrapulses with different modulations using a noncooperative method. Second, we obtained square matrices corresponding to various intrapulses by using the WVDs of signals and bicubic interpolation. Third, we randomly divided the dataset comprising the above square matrices into a training set, validation set, and test set. Finally, we used the proposed convolutional neural network (CNN) to evaluate the performance of the proposed IPR algorithm.

The contributions of this work are summarized as follows.

1) Bicubic interpolation was utilized to scale the initial WVD matrices into square matrices, which allowed radar intrapulses with different dimensions to be input into a fixed DNN model. As a result, the proposed method can process radar signals of varying lengths resulting from different sampling rates or PWs.
2) The proposed IPR algorithm via bicubic interpolation WVD demonstrated good performance and high robustness at a low signal-to-noise ratio (SNR) while maintaining a low time complexity. These characteristics met the requirements of rapid response in EW.
3) The intrapulse samples in the dataset used in experiments were generated by hardware equipment, which is more indicative of the reliability of the proposed method than the simulated samples.
4) The WVD square matrices, instead of images corresponding to WVDs, were directly used as the dataset. This approach prevented the loss of intrapulse features during the process of storing and reading images of WVDs.

The rest of this article is organized as follows. Section II describes related works. Section III introduces the dataset. Section IV provides the details of the proposed IPR algorithm. Section V discusses the experiments. Finally, Section VI concludes this article.

II. RELATED WORKS

A. Radar Intrapulse Preprocessing Theories

To acquire clearer features of radar intrapulses, domain transformation technologies, such as domain transforms, are often required. However, it is usually difficult to use a simple spectrogram to distinguish radar intrapulses. High-order spectra and cyclic spectra [30], [31], [32] are complicated and are not suitable for rapid response on the battlefields. Therefore, time–frequency analysis methods have become the most important and popular theory in domain transformation technologies.

WVD is a nonlinear time–frequency analysis method with fine time–frequency aggregation, which is often used to analyze nonstationary signals. It is expressed as follows:

$$W_x(t,\omega) = \int_{-\infty}^{+\infty} x\left(t+\frac{\tau}{2}\right)x^*\left(t-\frac{\tau}{2}\right)e^{-j\omega\tau}\mathrm{d}\tau \tag{1}$$

where t denotes the time information, ω denotes the frequency information, $x(t)$ denotes the collected radar intrapulse, τ denotes the time delay, $*$ denotes the complex conjugate operator, and j denotes an imaginary number. Actually, WVD is the Fourier transform of the instantaneous autocorrelation of the original intrapulse. There are also some other typical time–frequency analysis methods, such as the smoothed pseudo-Wigner–Ville distribution

(SPWVD), the CWD, the continuous wavelet transform (CWT), the synchronous wavelet transform (SWT), and the HHT. The SPWVD is expressed as follows:

$$\mathrm{SPW}_x(t,\omega)=\int_{-\infty}^{+\infty}h(\tau)\int_{-\infty}^{+\infty}g(u-\tau)\times x\left(t-u+\frac{\tau}{2}\right)x^*\left(t-u-\frac{\tau}{2}\right)e^{-j\omega t}\mathrm{d}u\mathrm{d}\tau \tag{2}$$

where $h(\tau)$ denotes a window function, and $g(u)$ denotes a smoothing function. The CWD is expressed as follows:

$$\mathrm{CW}_x(t,\omega)=\frac{1}{4\pi^{3/2}}\iint\frac{1}{\sqrt{\tau^2/\sigma}}e^{\frac{-\sigma(t-u)^2}{4\tau^2}}\times x\left(u+\frac{\tau}{2}\right)x^*\left(u-\frac{\tau}{2}\right)e^{-j\omega t}\mathrm{d}u\mathrm{d}\tau \tag{3}$$

where σ is a constant. The SPWVD and CWD are able to reduce the cross interference of the WVD, but this comes at the cost of sacrificing some of the time–frequency aggregations of the WVD. The CWT is expressed as follows:

$$\mathrm{CWT}_x(a,b)=\frac{1}{\sqrt{a}}\int_0^T x(t)\psi\left(\frac{t-b}{a}\right)\mathrm{d}t \tag{4}$$

where a is the scale factor, b is the time-shift factor, T represents the duration of signal $x(t)$, and $\psi(t)$ is the wavelet function. The performance of the CWT is easily affected by the selection of wavelet function. The SWT is expressed as follows:

$$\mathrm{SWT}_x(\omega_l,b)=\frac{1}{\Delta\omega}\sum_{a_k:|\omega(a,b)-\omega_l|\le\frac{\Delta\omega}{2}}\mathrm{CWT}_x(a,b)a_k^{-\frac{3}{2}}\Delta a_k \tag{5}$$

where ω_l denotes the frequency information, b denotes the time information, $\Delta\omega$ is the compression step for frequency redistribution, $\Delta\omega=\omega_l-\omega_{l-1}$, a_k is the discrete scale factor, $\Delta a_k=a_k-a_{k-1}$, k is the number of scales, and ":" means to make a certain condition true. Additionally, $\omega(a,b)$ is the instantaneous frequency, as shown in the following equation:

$$\omega(a,b)=\frac{-j}{2\pi\mathrm{CWT}_x(a,b)}\frac{\partial\mathrm{CWT}_x(a,b)}{\partial b} \tag{6}$$

where j denotes an imaginary number, and $\mathrm{CWT}_x(a,b)$ can be obtained by (4). The SWT is known to be sensitive to noise and may experience time–frequency divergence when processing complex-modulated signals. The HHT, on the other hand, involves several steps. First, the intrinsic-mode function (IMF) components are obtained by processing the radar intrapulses via the empirical-mode decomposition [33]. Second, the IMFs are processed by the Hilbert transform. Finally, the instantaneous frequency and amplitude of the intrapulses can be obtained.

Different time–frequency transforms correspond to different representations of radar intrapulses, and all of these transforms can be used in combination with bicubic interpolation. However, as bicubic interpolation may generate overshoots and undershoots, it is important to investigate which time–frequency transform is best suited for use with this type of interpolation. Therefore, the IPR system can achieve optimal performance by combining the most suitable time–frequency transform with bicubic interpolation.

B. Bicubic Interpolation

In a real-world radar intrapulse processing system, domain transformations are used to preprocess pulses with varying dimensions, which can result in matrices with different dimensions. This makes it challenging for a fixed CNN to accurately recognize these intrapulses. However, if bicubic interpolation is applied to process matrices with different dimensions into matrices with the same dimension, a fixed CNN can effectively identify signals with varying dimensions [34].

The bicubic interpolation method utilizes 16 closest neighboring points to the sampling point for interpolation. It is supposed that the dimension of the wanted matrix **B** is (M_1, M_2), and the dimension of the source matrix **A** is (m_1, m_2). Therefore, the scaling factor **k** is obtained via $\mathbf{k}=(k_1,k_2)=(M_1/m_1, M_2/m_2)$. The bicubic function is shown as follows:

$$W(x)=\begin{cases}(a+2)|x|^3-(a+3)|x|^2+1, & |x|\le 1\\ a|x|^3-5a|x|^2+8a\,|x|-4a, & 1<|x|<2\\ 0, & \text{otherwise}\end{cases} \tag{7}$$

where a is set to -0.5.

The steps of bicubic interpolation are as follows.

1) The arbitrary coordinate of **B** is assumed to be (X, Y). Then, the scaling factor **k** is calculated according to the dimension of the source matrix **A**. The corresponding coordinate (x, y) in **A** is equal to $(X/k_1, Y/k_2)$.
2) The nearest 16 coordinates (x_r, y_c) to (x, y) in **A** are obtained, where $r, c \in \{0, 1, 2, 3\}$.
3) The value corresponding to the coordinate (X, Y) of **B** can be obtained according to the following equation:

$$f(X,Y)=\sum_{r=0}^{3}\sum_{c=0}^{3}f(x_r,y_c)W(x-x_r)W(y-y_c) \tag{8}$$

where $f(x_r, y_c)$ represents the values corresponding to the coordinate (x_r, y_c) in **A**.

C. Similar Related Works

There have been some published materials on a similar topic of radar IPR. Cai et al. [35] utilized STFT to convert signals into images and then used three types of CNNs to extract features of the STFT images. While their contributions focused on improving the CNN, the details of signal processing were not very clear. Wu et al. [36] introduced the process of the recognition algorithm in detail, particularly the signal processing aspect. STFT images of

signals were used as a dataset to train the CNN, but no comparison was made between the performance of the STFT and other signal transformations, such as WVD and HHT. In [37], [38], and [39], an algorithm based on the fusion of features extracted by a CNN and a local binary pattern was proposed for modulation classification. SPWVD was used to preprocess signals. However, principal component analysis was applied in the algorithm, resulting in the loss of some cryptic features of the signals. Some other works also used SPWVD or fractional low-order CWDs combined with CNNs to achieve signal classification. However, they did not provide details on how signals were made into the dataset [40], [41]. Qu et al. [42], [43] used Cohen class time–frequency distribution, image processing techniques, and CNNs to identify the modulation of radar signals. A novel kernel function was developed to remove cross terms of WVD, and 2-D Wiener filtering was used to reduce the noise of time–frequency images (TFIs). Qu also used the Otsu method to transform TFIs into binary images and remove noise from the TFIs. The accuracy of their proposed method for recognizing 12 kinds of signals reached 96.1% when the SNR was −6 dB. However, Qu used bilinear interpolation to resize the TFIs and adopted binary TFIs, which led to the loss of some essential features of TFIs. In contrast, our work utilizes bicubic interpolation, which has better performance than bilinear interpolation [34], [44], and the values in the WVD matrix are not binary, thereby retaining more features of signals.

III. DATASET

A. Intrapulse Samples

In this work, six kinds of radar pulses with intermediate frequencies are generated by the hardware equipment of our project team. The radar pulses with different modulations are used as our research subject, and we construct the dataset for the IPR of radar signals using these radar pulses. Therefore, different radar intrapulses have different modulations. The above radar intrapulse modulations include binary phase-shift keying (BPSK), frequency encoding (FE), LFM, nonlinear frequency modulation (NLFM), CP, and quaternary phase-shift keying (QPSK). The PWs of the above intrapulses are 10 μs, the pulse period is 30 μs, and the carrier frequency F_0 is 20 MHz. Additionally, the chip durations of the modulations for BPSK are all 0.77 μs. FE modulation transmits at different frequencies with equal durations during the PW. The lowest and highest frequencies of LFM and NLFM modulation are 17.5 MHz and 22.5 MHz, respectively. The chip durations of the modulations for QPSK are all 0.77 μs. The details of intrapulse modulation parameters are shown in Table I.

For BPSK, if the phase of the unmodulated carrier is 0, the absolute codes 0 and 1, respectively, mean that the phases of the modulated carrier are 0 and π. And the relative codes 0 and 1, respectively, mean that the phase difference between the previous code and the next code is 0 and π. For QPSK, if the phase of the unmodulated carrier is 0, the absolute codes 0, 1, 2, and 3, respectively, mean that the phases of the modulated carrier are 0, $\pi/2$, π, and $3\pi/2$. And the relative codes 0, 1, 2, and 3, respectively, mean that the phase difference between the previous code and the following code is 0, $\pi/2$, π, and $3\pi/2$. These radar intrapulses are intercepted by the signal collector via a transmission wire. And the number of sampling points, which is a parameter in the signal collector, is set to 3 800 000. The sampling rate F_s is set to 50 MHz. Additionally, the pulse period of all radar signals is 30 μs.

TABLE I
Details of Intrapulse Modulation Parameters

Signal	Modulation information
BPSK	Absolute codes: 0101001100000 Relative codes: 0111101010000
FE	Carrier frequencies: 16, 19, 21, 24 MHz
LFM	Bandwidth: 5 MHz
NLFM	Bandwidth: 5 MHz
CP	--
QPSK	Absolute codes: 0132213201002 Relative codes: 0123032321302

- Absolute code means the phase difference between the modulated carrier and the unmodulated carrier.
- Relative code means the phase difference between the previous code and the following symbol.

B. Radar Intrapulse Processing

The process of obtaining the WVD square matrix involves three steps. First, the initial WVD matrix of the intercepted radar intrapulse is acquired. Second, the square matrix is obtained by using bicubic interpolation. Finally, the square matrices that make up the dataset are normalized to a maximum magnitude of 1. The process of obtaining the WVD square matrix is illustrated in Fig. 1.

WVD is a technique that converts a 1-D radar signal into a 2-D matrix. The resulting matrix is a complex matrix with a dimension of 500×1000, where 500 represents the number of rows of the initial WVD matrix with 500 sampling points, with each point representing different time information at the same frequency point. Similarly, 1000 represents the number of columns of the initial WVD matrix with 1000 sampling points, with each point representing different frequency information at the same time point. To simplify the calculation, we take the absolute value of each element in the matrix. Bicubic interpolation is then used to transform the matrix into a square matrix with a desired dimension of 500×500, determined by the maximum memory of our computer. This square matrix is obtained using the method, as described in Section II-B. Finally, to eliminate the influence of the amplitude of radar signals, we normalize the square matrix by scaling the maximum value to 1.

Using this approach, the recognition of radar intrapulses can be treated as a computer vision recognition problem. In our work, we directly use the WVD square matrices as inputs to the CNN, rather than using their corresponding

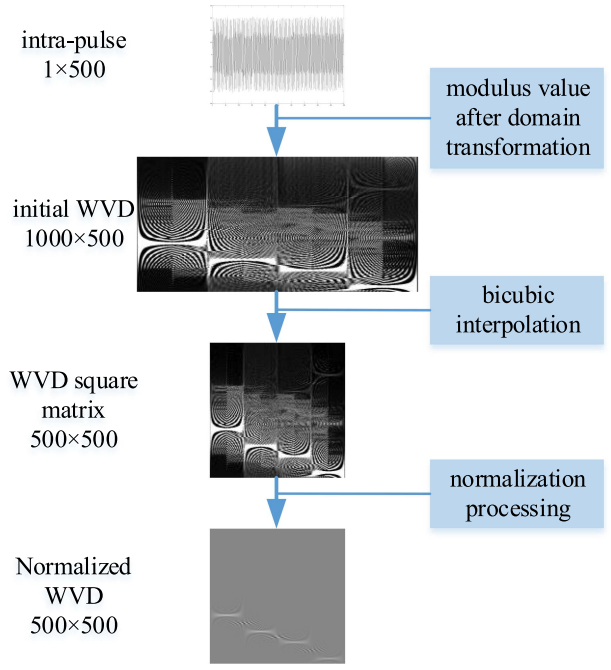

Fig. 1. Process of obtaining the WVD square matrix.

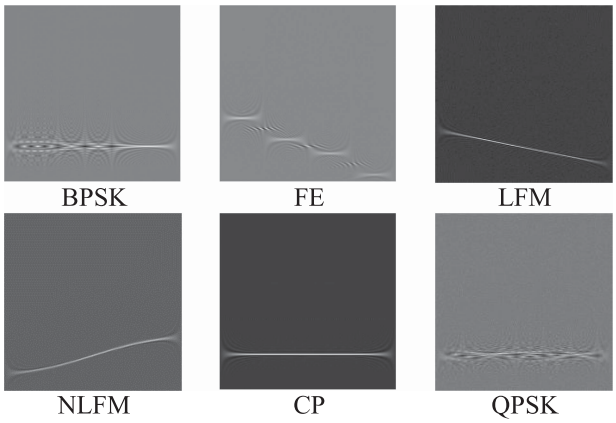

Fig. 2. Images corresponding to WVD square matrices of different radar intrapulses.

images. This is because the WVD images automatically saved by the software may lose some essential features of radar signals, which can adversely impact the performance of the trained CNN.

Fig. 2 shows the images corresponding to WVD square matrices of different radar intrapulses.

Fig. 2 illustrates that the WVD square matrices of different intrapulse signals can be utilized to recognize intrapulses. Although the BPSK and QPSK images shown above are slightly similar, they can still be effectively distinguished.

In this work, the signal collector can obtain at least 500 radar intrapulses of each class according to the 3 800 000 sampling points. Hence, there are all 3000 samples in the WVD square matrix dataset.

IV. METHOD

A. Convolutional Neural Network

CNNs are an essential model in computer vision and are particularly suitable for distinguishing WVD square matrices of radar intrapulses [45]. The structure of the CNN used in this work is shown in Fig. 3.

In Fig. 3, the numbers on top of the feature map represent the size of the feature map, such as "500^2." The numbers below the feature map represent the number of channels in the feature map, such as "15." The "Convolution(15, 3, 3, 'same')" indicates that the number and size of the convolution kernel are 15 and 3×3, respectively, and "same" stands for the zero-filling operation. The "Maxpooling(2, 2, s(2), 'same')" indicates that the pooling size is 2×2 and the stride is 2. "BatchNormalization" represents the batch normalization operation before the nonlinear activation function. Compared with the CNN model presented in our previous basic work [46], the proposed CNN in this work has a larger input size, as larger samples can contain more essential features of raw signals and help to reduce the impact of frequency cross-interference terms. Moreover, the number of neurons in the fully connected layer of the proposed CNN in this work is smaller as we have introduced batch normalization techniques. In this case, a smaller number of neurons do not affect the performance of the model but instead can reduce the complexity of the CNN. Furthermore, batch normalization techniques can speed up training and alleviate overfitting.

To improve the performance of the CNN, speed up the training process, and prevent overfitting, the following improvements were made in this study.

1) The trained network model with better recognition performance on the validation set was saved in real time.
2) Batch normalization was used before the nonlinear activation in the fully connected layer.
3) One-hot encoding technology was used to encode labels, making the feature distance more appropriate.

B. IPR Algorithm

The proposed IPR algorithm is divided into the stage of training the CNN model and the stage of identifying the radar signals. The block diagram representing the training of CNN model is shown in Fig. 4.

The block diagram representing the recognition of radar intrapulses is shown in Fig. 5. First, an intercepted intrapulse is preprocessed into a WVD square matrix. Second, the saved CNN model is loaded with the best performance. Third, the square matrix to be identified is inputted into the above model. Finally, the CNN model outputs the class of the radar intrapulse.

V. EXPERIMENTS

The experimental environment consists of Windows 10; GPU (NVIDIA GeForce RTX 3090); and CPU (Intel(R) Core(TM) i9-12900KF).

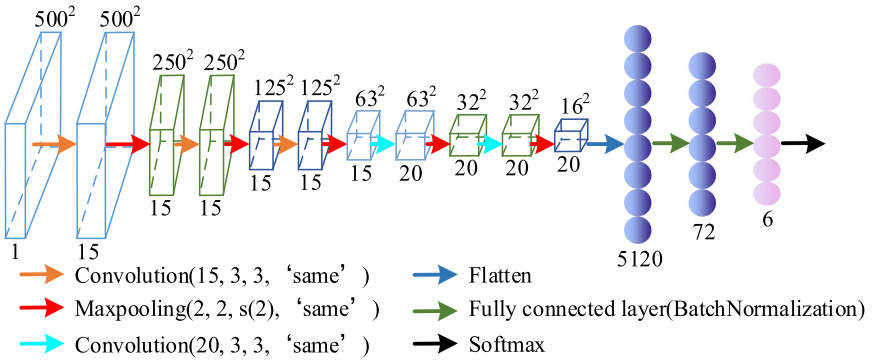

Fig. 3. Structure of the CNN used in this work.

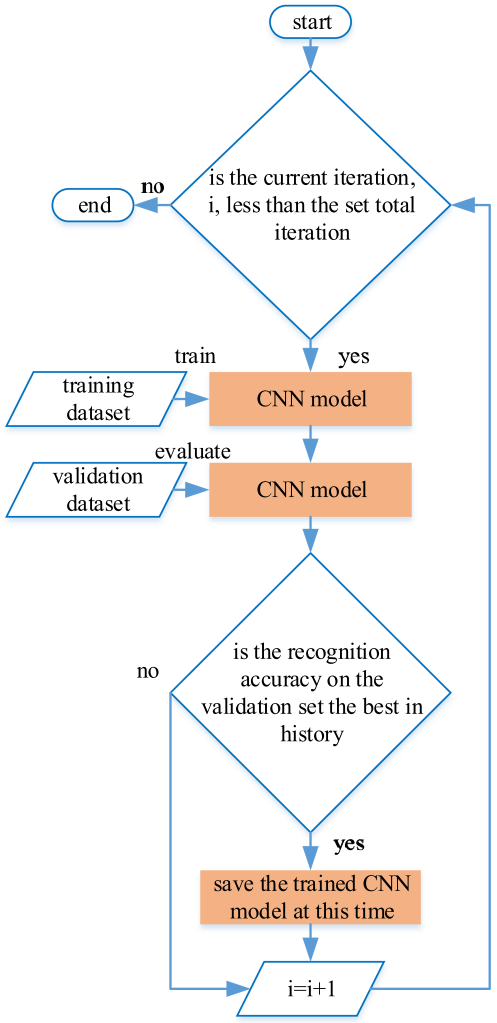

Fig. 4. Block diagram representing training of CNN model.

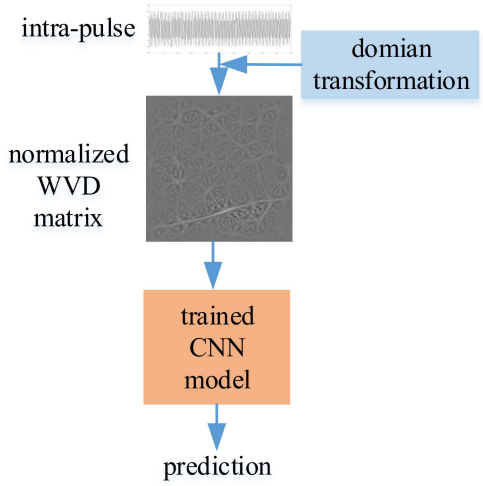

Fig. 5. Block diagram representing recognition of an intrapulse.

A. Performance Comparison of IPR Algorithms Based on Different Interpolation Methods

Apart from bicubic interpolation, the nearest neighbor interpolation method and the bilinear interpolation method can also process the initial WVD matrix into a square matrix. When the SNR is −8 dB, the resulting time–frequency WVD matrix images obtained by the nearest neighbor, bilinear, and bicubic interpolation schemes are shown in Fig. 6.

As shown in Fig. 6, the differences between the six types of intrapulses in Fig. 6(c) are more apparent than those in Fig. 6(a) and (b). Furthermore, Fig. 6 shows that the bicubic interpolation used is more suitable for resizing initial WVD matrices due to its higher quality than the nearest neighbor and bilinear interpolation. The dataset used in our subsequent experiments is not constructed based on the grayscale images, as shown in Fig. 6, but directly based on the WVD square matrices, which are saved as a mat format file. In fact, when the SNR is less than −10 dB, the recognition accuracy of the CNN model trained using grayscale images is 5% lower than that of the CNN model trained directly using WVD matrices. We presented Fig. 6 to highlight the advantages of bicubic interpolation more intuitively, and we plan to further demonstrate its advantages through experiments.

Specifically, the following experiment explores the performance of IPR algorithms based on different interpolation methods, and the WVD matrix processed by different interpolation methods still needs to be normalized, as shown in Fig. 1. The global parameters of the CNN throughout the study are set as follows: the number of training epochs

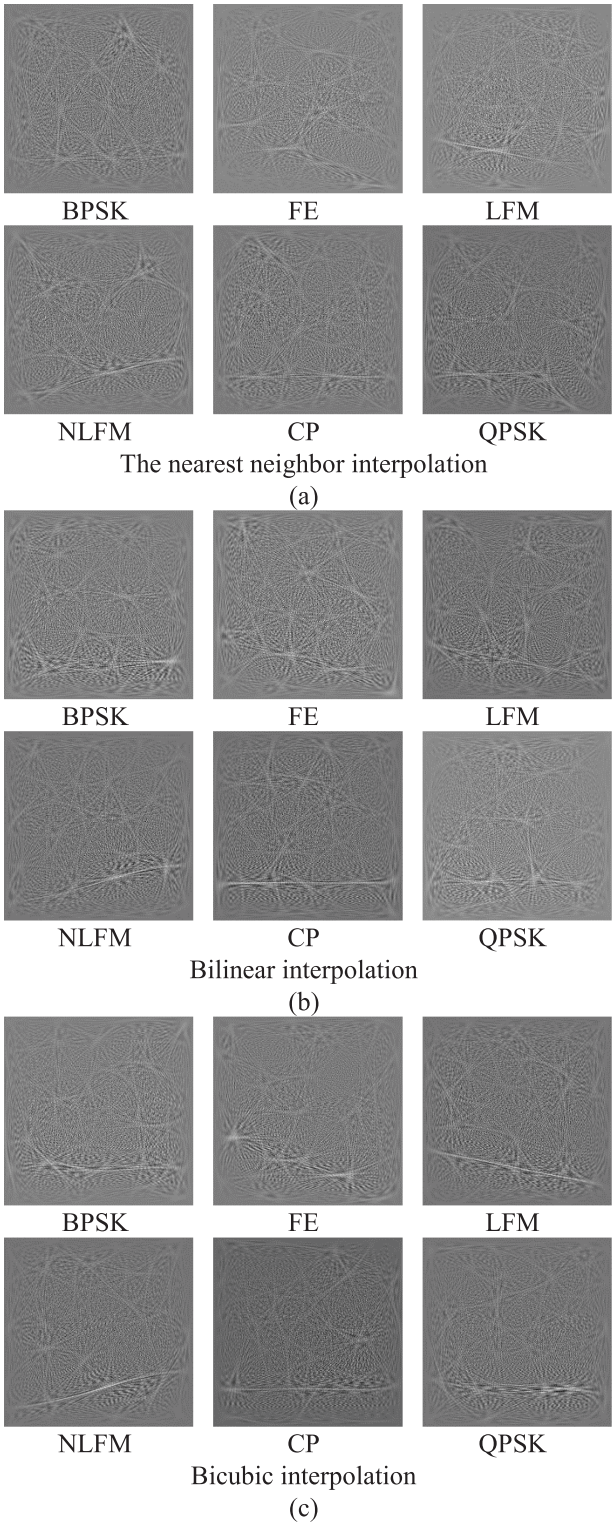

Fig. 6. Time–frequency WVD matrix images obtained by three interpolation schemes.

is 100, the batch size is 8, and the Adam optimizer is used. Each experiment is repeated 20 times, and the average result of the 20 experiments is used to represent the performance of various methods. The 20 experiments are independent of each other, so the average result can more accurately represent the performance of various methods. Furthermore, all experiments in this work were repeated 20 times independently to make the results more representative. Additionally, Gaussian noise is added to the radar pulses to obtain intrapulses with different SNRs.

From the 3000 radar intrapulses, 1800 intrapulses were randomly selected as the training set, 600 were randomly selected as the validation set, and the remaining 600 were used as the test set. The training set and the validation set were used to train the CNN. Unless, otherwise, specified, the training set, validation set, and test set for all subsequent sections are described above. Under different SNR conditions, for the test set, the average recognition accuracy of IPR algorithms based on different interpolation methods is shown in Fig. 7. The experiment was repeated 20 times independently to ensure the results representative.

As shown in Fig. 7, when the SNR is less than -6 dB, the recognition accuracy of IPR algorithms based on the nearest neighbor interpolation and bilinear interpolation is very low. Meanwhile, the accuracy based on bicubic interpolation is relatively high even when the SNR is only greater than -12 dB. This indicates that the nearest neighbor and bilinear interpolation lose more deep features than bicubic interpolation. Additionally, when the SNR is -4 dB, the recognition accuracy of the IPR algorithm based on the nearest neighbor or bilinear interpolation is close to 100%. However, when the SNR is -8 dB, the accuracy based on bicubic interpolation is already close to 100%. These results demonstrate that bicubic interpolation is more suitable for preprocessing the WVD matrix than nearest neighbor and bilinear interpolation.

B. Performance Comparison of IPR Algorithms Based on Different Domain Transformations

The reason why WVD rather than other domain transformations is chosen for preprocessing signal is that WVD can retain more deep characteristics at different SNR levels. While SPWVD, CWD, CWT, SWT, and HHT can also be used for preprocessing signals, they have different abilities to express time–frequency information and suppress noise. All of the above domain transformations are first used to preprocess signals, then the results obtained by the transformations are further processed by bicubic interpolation. The details regarding parameters configured for different domain transformation methods are shown in Table II.

By using different domain transformations and bicubic interpolation, various intrapulses can be recognized.

Under different SNR conditions, for the test set, the average recognition accuracy of IPR algorithms based on different domain transformations is shown in Fig. 8. The experiment was repeated 20 times independently to ensure the results representative.

Fig. 8 shows that the performance of the algorithm based on CWD is the closest to that based on WVD, and the performance of the algorithm based on SPWVD is slightly worse than those based on WVD and CWD. When the SNR is greater than -6 dB, the recognition accuracy of

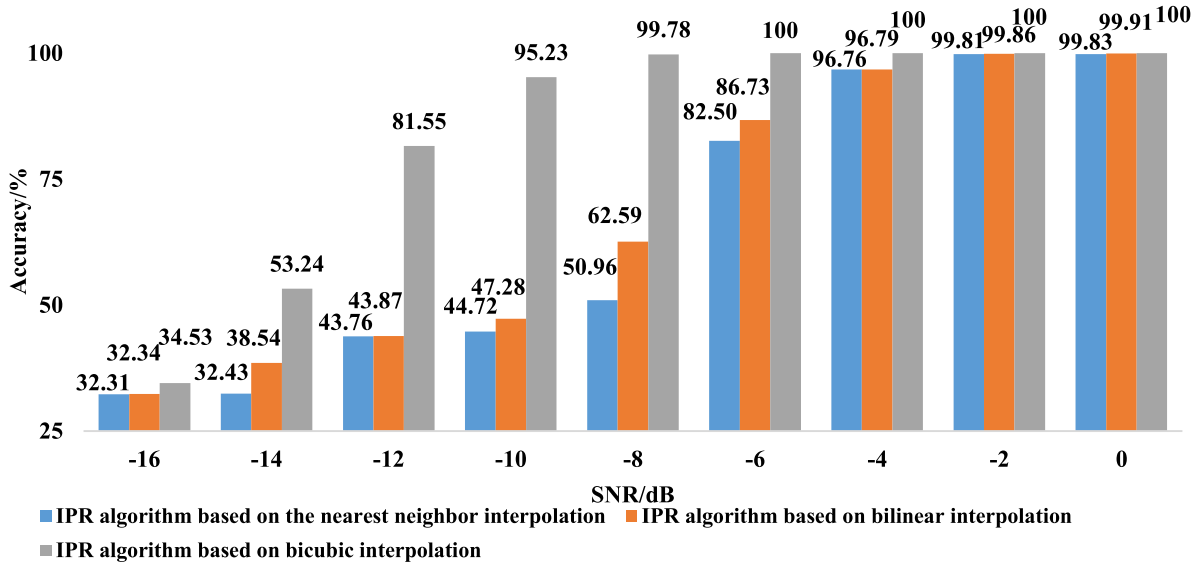

Fig. 7. Average recognition accuracy of IPR algorithms based on different interpolation methods (%).

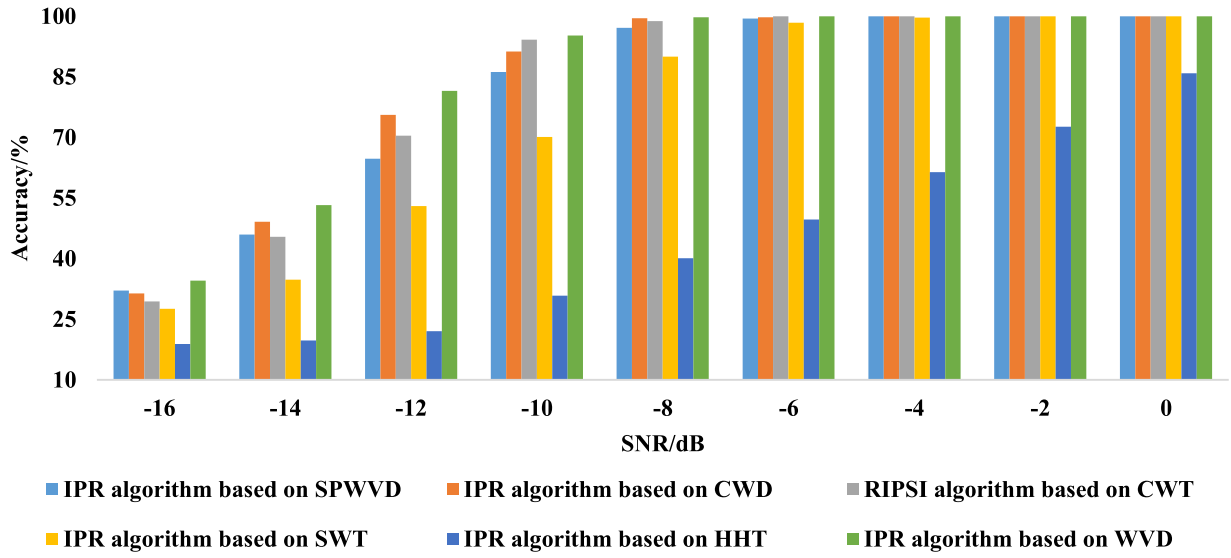

Fig. 8. Average recognition accuracy of IPR algorithms based on different domain transformations (%).

algorithms based on SPWVD, CWD, and WVD can almost reach 100%. This occurs because these three transformations belong to Cohen time–frequency distribution and have similar performance when SNR is high. SPWVD and CWD are mainly used to suppress cross-term interference of WVD by sacrificing their time–frequency aggregation. However, the experimental results show that WVD is more suitable than SPWVD and CWD for preprocessing signals under low SNR conditions due to its better time–frequency aggregation.

When SNR is less than −12dB, the recognition accuracy of algorithms based on CWT, SWT, and HHT transformations is less than 71%. Additionally, the CWT provides a "time–frequency" window that changes with frequency, which can have good time resolution for high frequency and good frequency resolution for low frequency. Hence, the CWT may lead to better recognition accuracy than some of the WVD-related transformations, especially when the SNR is greater than −12 dB. However, the intermediate frequency of radar signal is generally high, and the CWT would have low-frequency resolution, while having high time resolution. Furthermore, the selection of wavelet basis functions is very difficult, which greatly affects the wide use of CWT.

In summary, WVD feature transformation can preserve more essential features of radar intrapulses than other domain transformations. Hence, WVD is chosen for preprocessing signal in this work, and the performance of the IPR algorithm based on WVD is better than those based on other domain transformations.

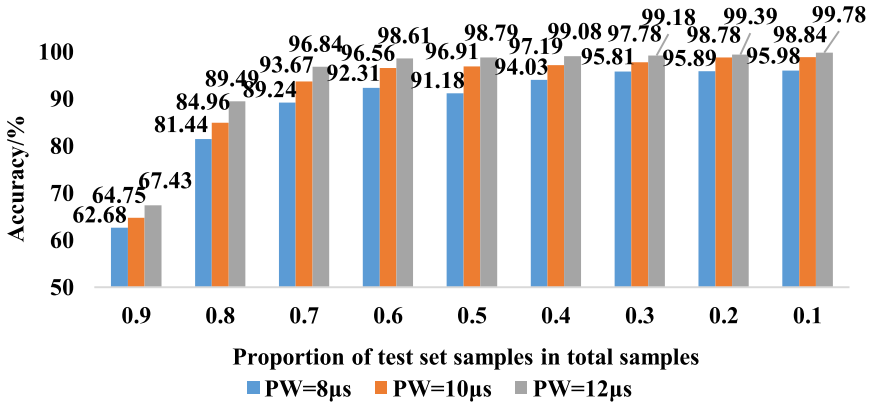

Fig. 9. Average recognition accuracy of IPR algorithm for intrapulses with different PWs (%).

TABLE II
Details Regarding Parameters Configured for Different Domain Transformation Methods

Methods	Details
SPWVD	Kaiser window with $length = 51$ and $\beta = 20$ for time smoothing, Kaiser window with $length = 125$ and $\beta = 20$ for frequency smoothing.
CWD	Kaiser window with $length = 51$ and $\beta = 20$ for time smoothing, Kaiser window with $length = 125$ and $\beta = 20$ for frequency smoothing, kernel function $g(\theta,\tau) = \exp(-\theta^2\tau^2/3.6)$.
CWT	Bump wavelet, the number of voices per octave is 48.
SWT	Bump wavelet, the number of voices per octave is 48.
HHT	The sift relative tolerance is 0.001, the sift max iterations is 1000, and the max number of IMF is 501.

C. Adaptability of IPR Algorithm

The most important and novel part of the proposed IPR algorithm is the use of bicubic interpolation to obtain a constant size feature matrix. The number of analog-to-digital converter sampling points varies with changes in the PW of different radars or in the sampling rate of the receiver. Without a constant size feature matrix, it would be challenging to train a fixed network using radar intrapulses with different PWs. However, bicubic interpolation can solve these problems, making the proposed IPR algorithm more adaptable to different radar intrapulses.

The six kinds of radar intrapulses, as shown in Table I, were still collected by the receiver, and the sampling rate was set to 62.5 MHz. All kinds of pulses with PW values of 8, 10, and 12 μs were acquired. When the SNR is -10 dB, the average recognition accuracy of the IPR algorithm for intrapulses with different PWs is shown in Fig. 9. The experiment was repeated 20 times independently to ensure the results representative.

As shown in Fig. 9, when the proportion is smaller than 0.7, the average recognition accuracy of the IPR algorithm for intrapulses with various PWs is almost over 90%, indicating that the proposed algorithm has better adaptability to radar intrapulses with different PWs. Additionally, the accuracies of the algorithm for intrapulses with larger PWs are higher. The WVD feature matrix obtained by an intrapulse with a larger PW will contain more characteristics of the radar signal, which helps to recognize radar intrapulses.

D. Comparative Experiments

The algorithm proposed in this work not only optimizes the basic CNN model but also optimizes the training strategy of the CNN model. The training strategy involves saving the CNNs with better performances during training. The end-to-end IPR algorithm based on a 1-D CNN [47] is also widely used due to its simplicity and intelligence. Additionally, there are methods that also use a combination of a time–frequency analysis method and bicubic interpolation, which are somewhat similar to the proposed method in this work, such as [42], [48], [49], and [50].

The basic CNN is somewhat similar to the improved CNN in Fig. 3. However, the key difference is that the basic CNN does not save the best performing model in real time during the training process on the validation set and does not utilize techniques, such as batch normalization and one-hot encoding. Additionally, the basic CNN is constructed with reference to LeNet-5 [51]. In the end-to-end IPR algorithm, the intercepted radar intrapulses are directly input to the 1-D CNN; thus, neither the WVD nor the interpolation scheme is used. The structure of the 1-D CNN in the end-to-end IPR algorithm is shown in Fig. 10.

In Fig. 10, the numbers on top of the feature map represent the size of the feature map, such as "500." The numbers below the feature map represent the number of channels in the feature map, such as "15." The "Convolution(15, 3, 'same')" indicates that the number of convolution kernels is 15, the size of the convolution kernel is 3×1, and "same" represents the zero-filling operation. The "Maxpooling(2,

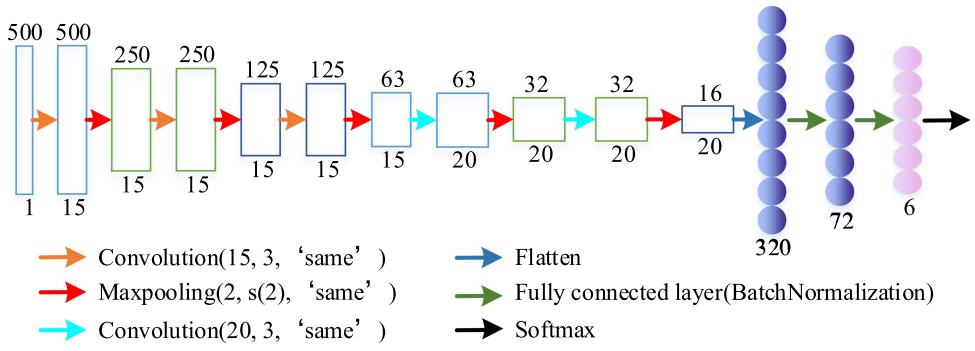

Fig. 10. Structure of a 1-D CNN in the end-to-end IPR algorithm.

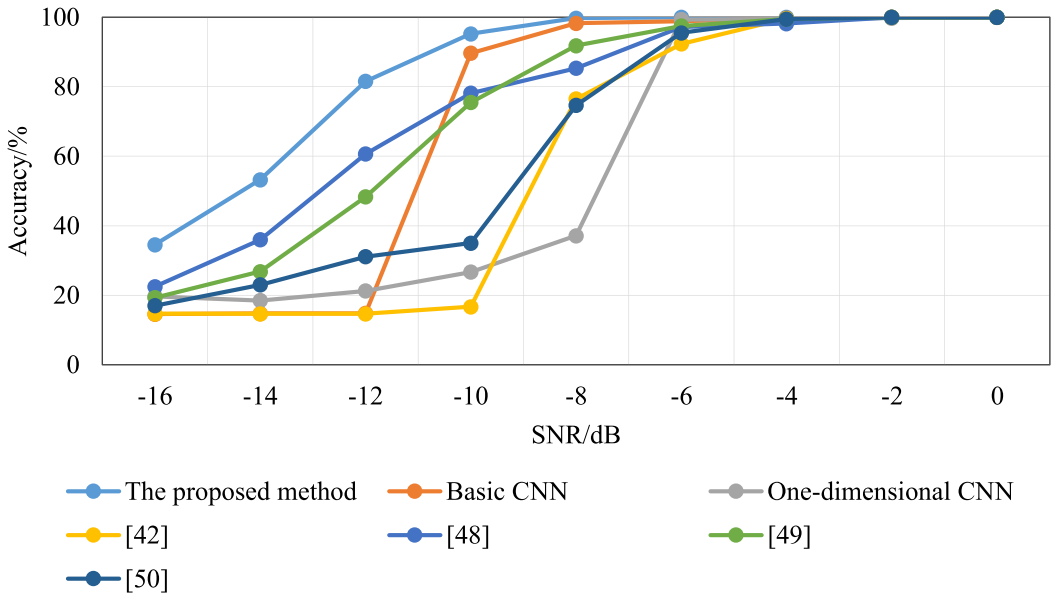

Fig. 11. Under different SNR conditions, the average recognition accuracies of different IPR algorithms(%).

s(2), 'same')" indicates that the pooling size is 2×1 and the stride is 2.

Under different SNR conditions, for the test set, the average recognition accuracy of different IPR algorithms is shown in Fig. 11. The experiment was repeated 20 times independently to make the results representative.

As shown in Fig. 11, all IPR algorithms struggle to effectively recognize intrapulses when the SNR is less than -12 dB. However, when the SNR is greater than -4 dB, all the algorithms can effectively recognize different intrapulses. Nonetheless, the performance of our method is superior to other methods under any SNR condition.

Fig. 11 shows that IPR algorithms based on the basic CNN and the 1-D CNN are more sensitive to changes in SNR. When the SNR changes slightly, such as from -12 to -10 dB or from -8 to -6 dB, the recognition accuracies of these two algorithms suddenly increase, indicating poor robustness. On the other hand, the performance of the proposed IPR algorithm steadily increases with an increase in SNR.

The performance of IPR algorithms based on [42], [48], [49], and [50] steadily improves as SNR increases, indicating that these methods are also not sensitive to SNRs. However, due to signal preprocessing or overly complex network models, these methods have not achieved better performance than our method. For instance, in [42], Wiener filtering, bilinear interpolation, and thresholding were applied to the CWD images of radar signals to remove noise and reduce complexity. However, applying too many processes may result in the loss of some important features.

Table III presents the time required for each method to train a sample, representing the time complexity of each method.

TABLE III
Time Required for Each Method to Train a Sample

Method	Our	Basic CNN	One-dimensional CNN	[42]
Time	0.174s	4s	0.003s	0.038s
Method	[48]	[49]	[50]	
Time	2s	5s	14s	

Table III presents that the proposed method, the 1-D CNN, and [42] have relatively low time complexity, while the time cost of basic CNN, [48], and [49] is high. The time cost of the method in [50] is the highest. A higher time cost implies a longer training process for the network. Such high time costs can be unfavorable for the practical application of signal recognition algorithms in EW.

In summary, improvements to the CNN model can enhance the recognition performance and robustness of the proposed IPR algorithm. Furthermore, the time complexity of the proposed IPR algorithm is not high, making it more adaptable to the demands of actual EW.

VI. CONCLUSION

An IPR algorithm based on bicubic interpolation WVD has been proposed to avoid the complexity of expert feature extraction in EW. Bicubic interpolation has improved the adaptability of the proposed algorithm to radar intrapulses with varying lengths. Experiments have shown that the proposed algorithm has outstanding recognition performance and good robustness, even under low SNR conditions. In the future, the following aspects would be focused on the following.

1) When the number of labeled different radar intrapulses is unbalanced, it can be difficult for the IPR algorithm to effectively recognize some classes of intrapulses.
2) When the number of intercepted labeled radar intrapulses is very small, it can be difficult for the IPR algorithm to recognize various intrapulses.
3) When radar signals are intercepted with no labels, an IPR algorithm for recognizing different intrapulses needs to be proposed.

REFERENCES

[1] U.S. Department of Defense, "Electromagnetic spectrum advantage strategy," Oct. 2020. [Online]. Available: https://media.defense.gov/2020/Oct/29/2002525927/-1/-1/0/ELECTROMAGNETIC_SPECTRUM_SUPERIORITY_STRATEGY.PDF

[2] M. E. Yıldırım, Y. B. Salman, and J.-S. Park, "Clustering for electronic warfare information," in *Proc. IEEE Conf. Control, Automat. Syst.*, 2018, pp. 1195–1197.

[3] Z. Xiao and Z. Yan, "Radar emitter identification based on novel time-frequency spectrum and convolutional neural network," *IEEE Commun. Lett.*, vol. 25, no. 8, pp. 2634–2638, Aug. 2021.

[4] G. Gok, Y. K. Alp, and O. Arikan, "A new method for specific emitter identification with results on real radar measurements," *IEEE Trans. Inf. Forensics Secur.*, vol. 15, pp. 3335–3346, Apr. 2020, doi: 10.1109/TIFS.2020.2988558.

[5] X. Wang, G. Huang, C. Ma, W. Tian, and J. Gao, "Convolutional neural network applied to specific emitter identification based on pulse waveform images," *IET Radar, Sonar Navig.*, vol. 14, no. 5, pp. 728–735, May 2020.

[6] L. Meng, W. Qu, and K. Cai, "Radar emitter identification based on stacked long and short term memory," in *Proc. Int. Conf. Adv. Mater, Electronical Mech. Eng.*, 2021, doi: 10.12783/dtmse/ameme2020/35532.

[7] S. Kuzdeba, A. Radlbeck, and M. Anderson, "Performance metrics for cognitive electronic warfare—Electronic support measures," in *Proc. IEEE Mil. Commun. Conf*, 2018, pp. 1–9, doi: 10.1109/MILCOM.2018.8599698.

[8] J. Matuszewski, "The analysis of modern radar signals parameters in electronic intelligence system," in *Proc. 13th Int. Conf. Modern Problems Radio Eng., Telecommun. Comput. Sci.*, 2016, pp. 298–302, doi: 10.1109/TCSET.2016.7452040.

[9] B. Park and J. M. Ahn, "Intra-pulse modulation recognition using pulse description words and complex waveforms," in *Proc. Int. Conf. Inf. Commun. Technol. Convergence*, 2017, pp. 555–560, doi: 10.1109/ICTC.2017.8191039.

[10] H. Q. Jiang, Z. Pang, P. Z. Tang, and L. Jia, "Intrapulse modulation recognition based on pulse description words," in *Proc. 6th Int. Congr. Image Signal Process.*, 2013, pp. 1367–1371, doi: 10.1109/CISP.2013.6743886.

[11] S. Wang and P. He, "Research on low intercepting radar waveform based on LFM and barker code composite modulation," in *Proc. Int. Conf. Sensor Netw. Signal Process.*, 2018, pp. 297–301, doi: 10.1109/SNSP.2018.00064.

[12] Y. Chunhong and L. Zengli, "The superiority analysis of linear frequency modulation and barker code composite radar signal," in *Proc. 9th Int. Conf. Comput. Intell. Secur.*, 2013, pp. 182–184, doi: 10.1109/CIS.2013.45.

[13] B. J. Skinner, J. P. Donohoe, and F. M. Ingels, "Correlation properties of Gaussian FSK/PSK radar signals," in *Proc. Southeastcon*, 1993, Paper 6, doi: 10.1109/SECON.1993.465734.

[14] J. Fernandes, M. Simsek, B. Kantarci, and S. Khan, "TableDet: An end-to-end deep learning approach for table detection and table image classification in data sheet images," *Neurocomputing*, vol. 468, pp. 317–334, 2022.

[15] Y. Gu, A. Chen, X. Zhang, C. Fan, K. Li, and J. S. Shen, "Deep learning based cell classification in imaging flow cytometer," *ASP Trans. Pattern Recognit. Intell. Syst.*, vol. 1, no. 2, pp. 18–27 , 2021.

[16] T. J. O'Shea, T. Roy, and T. C. Clancy, "Over-the-air deep learning based radio signal classification," *IEEE J. Sel. Topics Signal Process.*, vol. 12, no. 1, pp. 168–179, Feb. 2018, doi: 10.1109/JSTSP.2018.2797022.

[17] H. Zhou et al., "Few-shot electromagnetic signal classification: A data union augmentation method," *Chin. J. Aeronaut.*, vol. 35, pp. 49–57, 2022.

[18] S. H. Nawab and T. F. Quatieri, "Short-time Fourier transform," in *Advanced Topics in Signal Processing*. Englewood Cliffs, NJ, USA: Prentice-Hall, Sep. 1987, pp. 289–337.

[19] I. Daubechies, "The wavelet transform, time-frequency localization and signal analysis," *IEEE Trans. Inf. Theory*, vol. 36, no. 5, pp. 961–1005, Sep. 1990, doi: 10.1109/18.57199.

[20] B. Boashash and P. Black, "An efficient real-time implementation of the Wigner-Ville distribution," *IEEE Trans. Acoust., Speech, Signal Process.*, vol. 35, no. 11, pp. 1611–1618, Nov. 1987, doi: 10.1109/TASSP.1987.1165070.

[21] N. E. Huang and Z. H. Wu, "A review on Hilbert-Huang transform: Method and its applications to geophysical studies," *Rev. Geophys.*, vol. 46, no. 2, Jun. 2008, Art. no. RG2006.

[22] N. E. Huang, Z. Shen, and S. R. Long, "A new view of nonlinear water waves: The Hilbert spectrum," *Annu. Rev. Fluid Mech.*, vol. 31, no. 1, pp. 417–457, 1999.

[23] H.-I. Choi and W. J. Williams, "Improved time-frequency representation of multicomponent signals using exponential kernels," *IEEE Trans. Acoust., Speech, Signal Process.*, vol. 37, no. 6, pp. 862–871, Jun. 1989.

[24] Y. T. Feng, G. L. Wang, Z. P. Liu, R. M. Feng, X. Chen, and N. Tai, "An unknown radar emitter identification method based on semi-supervised and transfer learning," *Algorithms*, vol. 12, no. 12, Dec. 2019, Art. no. 271.

[25] C. Zhao, X. He, J. Liang, T. Wang, and C. Huang, "Radar HRRP target recognition via semi-supervised multi-task deep network," *IEEE Access*, vol. 7, pp. 114788–114794 , 2019.

[26] F. Ying and X. Wang, "Radar signal recognition based on modified semi-supervised SVM algorithm," in *Proc. IEEE 2nd Adv. Inf. Technol., Electron. Autom. Control Conf.*, 2017, pp. 2336–2340.

[27] J. Gong, X. Xu, and Y. Lei, "Unsupervised specific emitter identification method using radio-frequency fingerprint embedded InfoGAN," *IEEE Trans. Inf. Forensics Secur.*, vol. 15, pp. 2898–2913, Mar. 2020, doi: 10.1109/TIFS.2020.2978620.
[28] D. Marez, S. Borden, G. Clarke, J. Reeder, and N. Johnson, "Radar emitter and activity identification using deep clustering methods," *Proc. SPIE*, vol. 11006, 2019, Art. no. 110061H.
[29] M. W. Li, M. H. He, J. Han, and Y. W. Tang, "A new clustering and sorting algorithm for radar emitter signals," *J. Phys., Conf. Ser.*, vol. 1617, no. 1, Aug. 2020, Art. no. 012009.
[30] S. Fu and X. Liu, "A new method to solve the problem of facing less learning samples in signal modulation recognition," *EURASIP J. Wireless Commun. Netw.*, vol. 2020, Jan. 2020, Art. no. 8.
[31] D. Wang, N. Zhang, Z. Li, F. Gao, and X. Shen, "Leveraging high order cumulants for spectrum sensing and power recognition in cognitive radio networks," *IEEE Trans. Wireless Commun.*, vol. 17, no. 2, pp. 1298–1310, Feb. 2018, doi: 10.1109/TWC.2017.2777488.
[32] S. Liu, J. Shao, T. J. Kong, and R. Malekian, "ECG arrhythmia classification using high order spectrum and 2D graph Fourier transform," *Appl. Sci.*, vol. 10, no. 14, Jul. 2020, Art. no. 4741.
[33] N. E. Huang et al., "The empirical mode decomposition and the Hilbert spectrum for nonlinear and non-stationary time series analysis," *Proc. Roy. Soc. A, Math., Phys. Eng. Sci.*, vol. 454, pp. 903–995, 1971.
[34] R. Keys, "Cubic convolution interpolation for digital image processing," *IEEE Trans. Acoust., Speech, Signal Process.*, vol. 29, no. 6, pp. 1153–1160, Dec. 1981, doi: 10.1109/TASSP.1981.1163711.
[35] J. Cai, C. Li, and H. Zhang, "Modulation recognition of radar signal based on an improved CNN model," in *Proc. IEEE 7th Int. Conf. Comput. Sci. Netw. Technol.*, 2019, pp. 293–297, doi: 10.1109/ICCSNT47585.2019.8962418.
[36] J. Wu, Y. Zhong, and A. Chen, "Radio modulation classification using STFT spectrogram and CNN," in *Proc. 7th Int. Conf. Comput. Commun.*, 2021, pp. 178–182, doi: 10.1109/ICCC54389.2021.9674714.
[37] C. Hou, Y. Li, X. Chen, and J. Zhang, "Automatic modulation classification using KELM with joint features of CNN and LBP," *Phys. Commun.*, vol. 45, Apr. 2021, Art. no. 101259.
[38] C. Hou, C. Fang, Y. Lin, Y. Li, and J. Zhang, "Implementation of a CNN identifying modulation signals on an embedded SoC," in *Proc. IEEE 63rd Int. Midwest Symp. Circuits Syst.*, 2020, pp. 490–493, doi: 10.1109/MWSCAS48704.2020.9184608.
[39] K. Li and J. Shi, "Modulation recognition algorithm based on digital communication signal time-frequency image," in *Proc. 8th Int. Conf. Dependable Syst. Appl.*, 2021, pp. 747–748, doi: 10.1109/DSA52907.2021.00114.
[40] M. Zhu, Y. Li, Z. Pan, and J. Yang, "Automatic modulation recognition of compound signals using a deep multi-label classifier: A case study with radar jamming signals," *Signal Process.*, vol. 169, Apr. 2020, Art. no. 107393.
[41] X. Tian, X. Sun, X. Yu, and X. Li, "Modulation pattern recognition of communication signals based on fractional low-order Choi-Williams distribution and convolutional neural network in impulsive noise environment," in *Proc. IEEE 19th Int. Conf. Commun. Technol.*, 2019, pp. 188–192, doi: 10.1109/ICCT46805.2019.8947208.
[42] Z. Qu, X. Mao, and Z. Deng, "Radar signal intra-pulse modulation recognition based on convolutional neural network," *IEEE Access*, vol. 6, pp. 43874–43884, 2018, doi: 10.1109/ACCESS.2018.2864347.
[43] Z. Qu, Chenfan Hou, C. Hou, and W. Wang, "Radar signal intra-pulse modulation recognition based on convolutional neural network and deep Q-learning network," *IEEE Access*, vol. 8, pp. 49125–49136, 2020, doi: 10.1109/ACCESS.2020.2980363.
[44] S. Gao and V. Gruev, "Bilinear and bicubic interpolation methods for division of focal plane polarimeters," *Opt. Express*, vol. 19, pp. 26161–26173, 2011.
[45] S. L. Peng et al., "Modulation classification based on signal constellation diagrams and deep learning," *IEEE Trans. Neural Netw.*, vol. 30, no. 3, pp. 718–727, Mar. 2019, doi: 10.1109/TNNLS.2018.2850703.
[46] Z.-L. Wu, X.-X. Huang, M. Du, J.-F. Pan, and D.-P. Bi, "Intelligent identification of radar intra-pulse signals," *Proc. SPIE*, vol. 12169, 2022, Art. no. 121691Z.
[47] G. Shao, Y. Chen, and Y. Wei, "Convolutional neural network-based radar jamming signal classification with sufficient and limited samples," *IEEE Access*, vol. 8, pp. 80588–80598, 2020, doi: 10.1109/ACCESS.2020.2990629.
[48] Q. Tang, H.-H. Huang, and Z. Chen, "A novel approach for automatic recognition of LPI radar waveforms based on CNN and attention mechanisms," in *Proc. 41st Chin. Control Conf.*, 2022, pp. 6648–6653.
[49] H. Wu, C. Zhang, L. Shui, Y. Zhang, X. Li, and M. Lei, "Research on radar signal recognition technology based on residual convolutional neural network," in *Proc. 4th Int. Conf. Adv. Inf. Sci. Syst.*, 2022, pp. 1–6.
[50] Q. Li, W. Liu, C. Niu, Y. Bao, and Z. Hui, "Radar signal modulation recognition based on split EfficientNet under low signal-to-noise ratio," *Acta Electronica Sinica*, vol. 51, no. 3, pp. 675–686, 2023.
[51] Y. LeCun, L. Bottou, Y. Bengio, and P. Haffner, "Gradient-based learning applied to document recognition," *Proc. IEEE*, vol. 86, no. 11, pp. 2278–2324, Nov. 1998.

Zi-Long Wu was born in Huaibei, China, in 1998. He received the bachelor's degree in communication engineering from Xiamen University, Xiamen, China, in 2014, and the master's degree in information and communication engineering in 2018 from the National University of Defense Technology, Hefei, China, where he is currently working toward the Ph.D. degree in information and communication engineering.

His research interests include signal processing, deep learning, and radar recognition.

Xiang-Xuan Huang was born in 1995. He is currently working toward the master's degree with the National University of Defense Technology, Hefei, China.

His research interests include signal processing and fault detection.

Meng Du was born in Wuhan, China, in 1998. He received the bachelor's degree in information and communication engineering in 2020 from the National University of Defense Technology, Hefei, China, where he is currently working toward the master's degree in information and communication engineering.

His research interests include deep learning and radar countermeasures.

Xin-Song Xu received the bachelor's degree in information and communication engineering in 2012 from the National University of Defense Technology, Hefei, China, where he is currently working toward the Ph.D. degree in information and communication engineering.

His research interests include artificial intelligence and radar reconnaissance.

Daping Bi was born in Anhui in 1965. He received the bachelor's and master's degrees in information and communication engineering from the Electronic Engineering Institute of the People's Liberation Army, China, in 1987 and 1990, respectively.

He is currently a Professor and Doctoral Supervisor with the National University of Defense Technology, Hefei, China. His research interests include radar identification, radar imaging, and radar behavior recognition.

Ji-Fei Pan was born in Chuzhou, Anhui. He received the bachelor's, master's, and Ph.D. degrees in information and communication engineering from the Electronic Engineering Institute of the People's Liberation Army, China, in 2003, 2006, and 2009, respectively.

He is currently a Professor and Master's Supervisor with the National University of Defense Technology, Hefei, China. His research interests include radar emitter individual identification and electromagnetic warfare.